Structure and Conductivity of Small-Molecule Electrolytes $[CH_3O(CH_2CH_2O)_nCH_3]$:$LiAsF_6$ ($n = 8-12$)

Chuhong Zhang, Scott J. Lilley, David Ainsworth, Edward Staunton, Yuri G. Andreev, Alexandra M. Z. Slawin, and Peter G. Bruce*

EaStCHEM, School of Chemistry, The Purdie Building, University of St. Andrews, Fife KY16 9ST, United Kingdom

Received February 22, 2008. Revised Manuscript Received April 21, 2008. Accepted April 22, 2008

The crystal structures of $[CH_3O(CH_2CH_2O)_nCH_3]$:$LiAsF_6$ ($n = 8-12$) are reported. Each glyme forms a structurally unique complex with $LiAsF_6$. In all glymes Li^+ ions are six coordinated when only ether oxygens are involved in coordination. The coordination number is reduced to five when a fluorine from the AsF_6^- anion is involved in coordination. The absence of convenient pathways for Li^+ ions in the structures account for low lithium transport numbers ($t_+ < 0.3$) in the reported complexes, while greater distances between neighboring anions explain lower conductivities, compared with complexes prepared with lower glymes ($n = 3, 4$).

Introduction

The discovery of ionic conductivity in crystalline polymer/salt complexes has generated interest in determining the factors that influence their level of conductivity.[1] The crystal structure plays the decisive role. For example, complexes of α-PEO_6:$LiXF_6$ (X = P, As, Sb), in which Li^+ ions reside within continuous tunnels formed by poly(ethylene oxide) (PEO) chains and coordinated solely by ether oxygens, exhibit appreciable levels of conductivity, whereas β- PEO_6:$LiXF_6$ complexes do not.[2–5] Anionic doping, dispersity of the polymer chain lengths, the type of the chain ends, and the molecular weight of PEO have a pronounced effect on the conductivity of α-PEO_6:$LiXF_6$.[4,6–9] The structures of all known crystalline polymer electrolytes remains on reduction of the molecular weight of PEO, from millions to 1000 Da (chain lengths from thousands to 22 EO units). However, further reduction of the chain length, into the glyme range, leads to formation of complexes with entirely different crystal structures. It has been reported recently that these glyme:salt compounds form a new class of ionic conductors, small-molecule electrolytes, which are different from both ceramic and polymer electrolytes.[10]

A number of structures formed between Li salts and lower glymes, diglyme ($CH_3O(CH_2CH_2O)_2CH_3$), triglyme ($CH_3O(CH_2CH_2O)_3CH_3$), and tetraglyme ($CH_3O(CH_2CH_2O)_4CH_3$), have been determined as well as their phase behavior and crystallization kinetics.[11–16] Every glyme, when complexed with a lithium salt, forms a unique crystal structure with a specific EO:Li ratio.

In this paper we report several structures formed between $LiAsF_6$ and glymes with higher numbers of EO units: octaglyme (G8; $CH_3O(CH_2CH_2O)_8CH_3$), nonaglyme (G9; $CH_3O(CH_2CH_2O)_9CH_3$), undecaglyme (G11; $CH_3O(CH_2CH_2O)_{11}CH_3$), and dodecaglyme (G12; $CH_3O(CH_2CH_2O)_{12}CH_3$), which are closer in chain length to the low molecular weight crystalline polymer electrolytes.

Experimental Section

Glymes used for growing single crystals of the glyme:$LiAsF_6$ complexes were synthesized by replacing the hydroxy end groups of the corresponding glycols by methoxy groups using a modified Williamson ether synthesis.[17]

Octaethylene, nonaethylene, undecaethylene, and dodecaethylene glycols were supplied by Polypure. The resulting glymes were confirmed by matrix-assisted laser desorption ionization mass spectroscopy (MALDI-MS) to be free of unreacted dihydroxy-terminated glycols and monomethylated glycols. The MALDI mass

* To whom correspondence should be addressed.

(1) Gadjourova, Z.; Andreev, Y. G.; Tunstall, D. P.; Bruce, P. G. *Nature* **2001**, 412–520.
(2) MacGlashan, G. S.; Andreev, Y. G.; Bruce, P. G. *Nature* **1999**, *398*, 792.
(3) Gadjourova, Z.; Martin, D.; Andersen, K. H.; Andreev, Y. G.; Bruce, P. G. *Chem. Mater.* **2001**, *13*, 1282.
(4) Stoeva, Z.; Martin-Litas, I.; Staunton, E.; Andreev, Y. G.; Bruce, P. G. *J. Am. Chem. Soc.* **2003**, *125*, 4619.
(5) Staunton, E.; Andreev, Y. G.; Bruce, P. G. *J. Am. Chem. Soc.* **2005**, *127*, 12176.
(6) Christie, A. M.; Lilley, S. J.; Staunton, E.; Andreev, Y. G.; Bruce, P. G. *Nature* **2005**, *433*, 50.
(7) Zhang, C.; Staunton, E.; Andreev, Y. G.; Bruce, P. G. *J. Am. Chem. Soc.* **2005**, *127*, 18305.
(8) Lilley, S. J.; Andreev, Y. G.; Bruce, P. G. J. *Am. Chem. Soc.* **2006**, *128*, 12036.
(9) Staunton, E.; Andreev, Y. G.; Bruce, P. G. *Faraday Discuss.* **2007**, *134*, 143.
(10) Zhang, C.; Andreev, Y. G.; Bruce, P. G. *Angew. Chem., Int. Ed.* **2007**, *46*, 2848.
(11) Henderson, W. A.; Brooks, N. R.; Brennessel, W. W., Jr *Chem. Mater.* **2003**, *15*, 4679.
(12) Henderson, W. A.; Brooks, N. R., Jr *Chem. Mater.* **2003**, *15*, 4685.
(13) Seneviratne, V.; Frech, R.; Furneaux, J. E.; Khan, M. *J. Phys. Chem. B* **2004**, *108*, 8124.
(14) Andreev, Y. G.; Seneviratne, V.; Khan, M.; Henderson, W. A.; Frech, R.; Bruce, P. G. *Chem. Mater.* **2005**, *17*, 767.
(15) Henderson, W. A. *J. Phys. Chem. B* **2006**, *110*, 13177.
(16) Henderson, W. A. *Macromolecules* **2007**, *40*, 4963.
(17) Cooper, D. R.; Booth, C. *Polymer* **1977**, *18*, 164.

10.1021/cm8005327 CCC: $40.75
Published on Web 05/31/2008

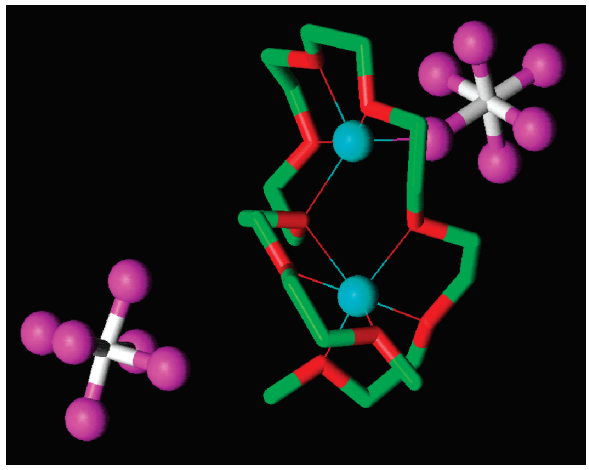

Figure 1. Local coordination environment of Li^+ ions in the structure of G8:$(LiAsF_6)_2$. Thin lines indicate coordination around the Li^+ cation. Hydrogens not shown.

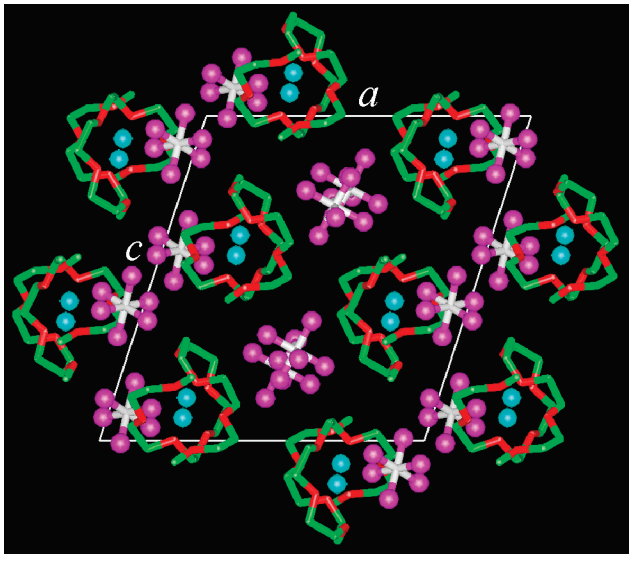

Figure 2. Structure of G8:$(LiAsF_6)_2$. Hydrogens not shown.

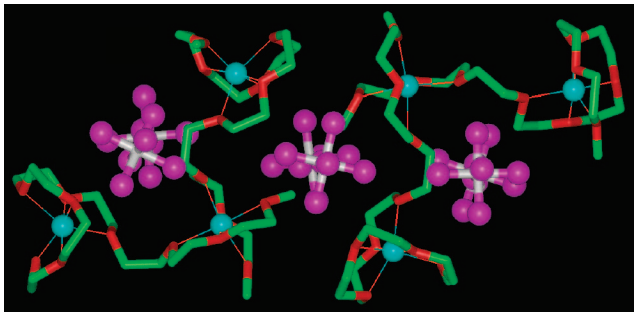

Figure 3. Local coordination environment of Li^+ ions in the structure of $(G8)_2$:$(LiAsF_6)_3$. Thin lines indicate coordination around the Li^+ cation. Hydrogens not shown.

spectra were collected on a Micromass TofSpec 2E spectrometer utilizing a 337 nm laser in reflection mode, and the sample was incorporated into the matrix via an aqueous solution.

Glymes were dried over 4 Å molecular sieves, and $LiAsF_6$ (ABCR, 99.8%) was dried at 50 °C for 24 h under dynamic vacuum before use. Preparation of the single crystals was carried out in a high-integrity argon-filled MBraun glovebox. First, appropriate quantities of $LiAsF_6$ and the corresponding glymes were dissolved in dry acetonitrile. G8 complex: G8 (0.301 g, 0.75 mmol), $LiAsF_6$ (0.222 g, 1.13 mmol) and G8 (0.305 g, 0.77 mmol), $LiAsF_6$ (0.150 g, 0.77 mmol). G9 complex: G9 (0.386 g, 0.87 mmol), $LiAsF_6$ (0.171 g, 0.87 mmol). G11 complex: G11 (0.282 g, 0.53 mmol), $LiAsF_6$ (0.208 g, 1.06 mmol). G12 complex: G12 (0.320 g, 0.56 mmol), $LiAsF_6$ (0.109 g, 0.56 mmol). After dissolution, the corresponding solutions for each complex were added together and transferred into glass vials. The solvent was allowed to evaporate slowly over molecular sieves. This led to formation of single crystals.

For conductivity measurements a self-supporting disk of each sample was placed into a two-electrode cell and sealed inside an argon-filled can. The can was then placed into a temperature-controlled oil bath. Conductivity data were obtained using ac impedance measurements carried out with a Solartron 1255 frequency response analyzer coupled with a Solartron 1286 electrochemical interface. Further details are available in ref 10. The measurements were carried out using ac impedance spectroscopy of sets of individually prepared samples for each complex.

Differential scanning calorimetry was carried out using a Netzch DSC 204 Phoenix with a heating rate of 10°/min using approximately 2 mg of each sample placed into an aluminum pan and sealed under Ar atmosphere.

Single-crystal X-ray diffraction data were collected at 93 or 173 K using a Rigaku MM007 high-brilliance RA generator (Mo Kα radiation or Cu Kα radiation, confocal optics) and either a Mercury CCD or a Saturn92 CCD system. At least a full hemisphere of data was collected using ω scans. Intensities were corrected for Lorentz polarization and absorption. The structures were solved by direct methods. Hydrogen atoms bound to carbon were idealized. Structural refinements were performed with full-matrix least squares based on F^2 using the program SHELXTL.[18] The largest size of single crystals that could be grown for some of the complexes was restricted to $0.1 \times 0.1 \times 0.01$ mm. This coupled with the fact that the crystals are composed of light atoms resulted in the agreement indices for some complexes being slightly in excess of 10%. However, the level of structural detail extracted and the key conclusions concerning structure/property relationships are in accord with the accuracy of the determinations.

Results and Discussion

Structure of Octaglyme Complexes. Depending on the molar ratio of octaglyme vs salt in the mixture (see Experimental Section), from which the single crystals were grown, either G8:$(LiAsF_6)_2$ or $(G8)_2$:$(LiAsF_6)_3$ complexes were formed.

G8:$(LiAsF_6)_2$. The oxygen to lithium ratio in this complex is 4.5:1. There are two crystallographically distinct lithium ions located in two different coordination environments, Figure 1. One lithium is coordinated by six ether oxygens of the octaglyme and the other by four oxygens from the same glyme and by a fluorine from an adjacent AsF_6^- ion. One ether oxygen coordinates both Li^+ ions, although it is closer to the anion-coordinated lithium ion (2.17 vs 2.59 Å). The rest of the lithium to oxygen distances are within the range 2.01−2.21 Å. With only one octaglyme coordinating both lithium ions the Li−Li distance within the solvate is short, 3.86 Å.

Figure 2 shows columns formed by the cation solvates (projected into page). The separation between lithium ions in the neighboring solvates along the column axis is 7.70 Å.

(18) Sheldrick, G. M. *SHELXTL 6.14*; Bruker AXS: Madison, 2004.

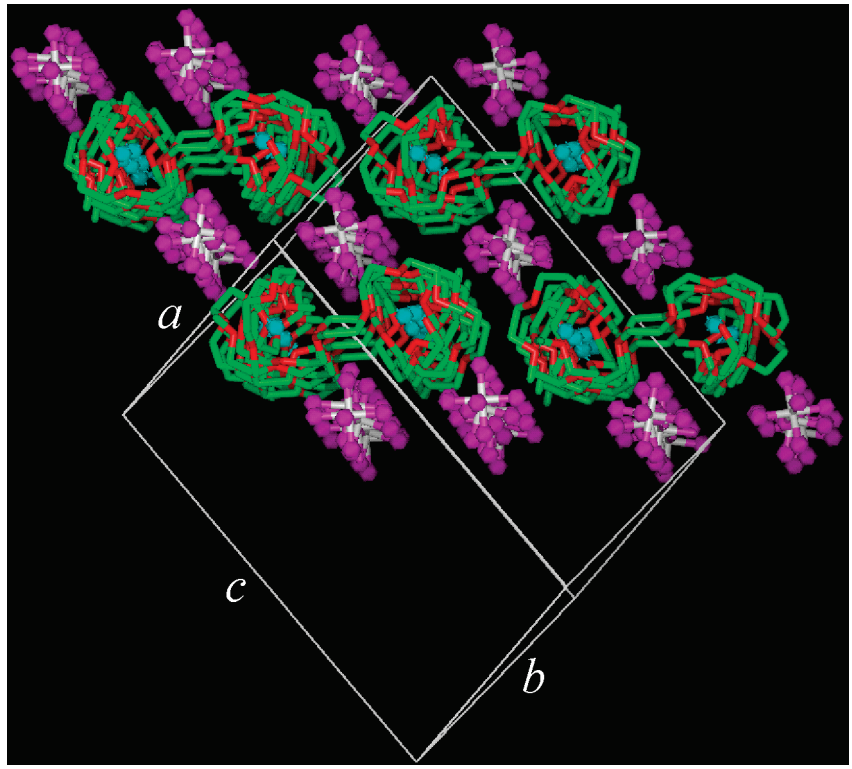

Figure 4. Structure of $(G8)_2$:$(LiAsF_6)_3$. Hydrogens not shown.

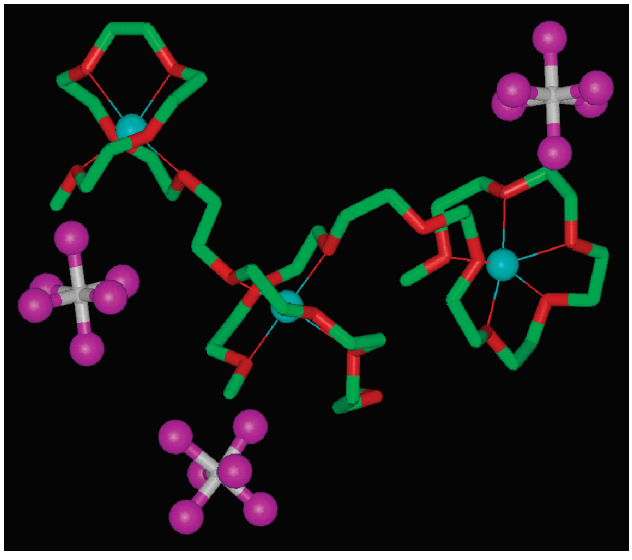

Figure 5. Local coordination environment of Li^+ ions in the structure of $(G9)_2$:$(LiAsF_6)_3$. Thin lines indicate coordination around the Li^+ cation. Hydrogens not shown.

The solvate columns are separated by columns of anions of two different types. One column comprises the anions, arranged in a zigzag pattern along the column axis, that coordinate the lithium ions, and another is formed by linearly stacked noncordinating anions. The distances between the lithium ions in neighboring columns take approximate values of 8.76, 9.23, and 11.72 Å. The narrowest dimension is short in comparison to the 9.21 Å separations of the Li^+ ions in the tunnels of PEO_6:$LiAsF_6$. The separations of arsenic atoms from their nearest neighbors moving along the column axis are 5.79 Å for the uncoordinated anions and 7.70 and 5.98 Å for the coordinated anions.

$(G8)_2$:$(LiAsF_6)_3$. The second octaglyme complex has an oxygen to lithium ratio of 6:1. There are six lithium ions in the asymmetric unit, each coordinated by six ether oxygens, with Li^+-O distances within the range 1.99−2.36 Å. To achieve this coordination, glymes and lithiums are arranged in two groups that are almost identical in shape, each comprising three Li^+ ions and two octaglyme molecules, Figure 3. Each octaglyme donates six end ether oxygens to create the coordination environment for one of the lithiums. The third lithium in the group bridges the two octaglymes and is coordinated by six remaining ether oxygens, three from each glyme. Each group adopts an L shape, with the shared Li^+ ion located in the corner. The two L-shaped groups are stacked in an S shape in the asymmetric unit (see Figure 3). The distances between nearest lithium ions, within each group and between the two groups, are in the range 6.43−7.44 Å. Only a single, the shortest, Li−Li distance (6.43 Å) in $(G8)_2$:$(LiAsF_6)_3$ is similar to that in PEO_6:$LiAsF_6$.

In the extended structure, Figure 4, S-shaped pairs of solvates interlock to form columns, with the latter arranged in rows. The solvate rows are separated by rows of columns formed by the AsF_6^- ions. The closest distance between Li^+ ions belonging to different solvate columns is 7.85 Å, both along and between the rows of columns. The anions are separated by 6.58−8.06 Å along the columns and 6.75−8.54 Å across the columns.

Structure of $(G9)_2$:$(LiAsF_6)_3$. The oxygen to lithium ratio in the nonaglyme complex is 6.7:1. Each of the three lithium ions in the asymmetric unit is coordinated by six ether oxygens, with Li^+-O distances being within the range 1.99−2.37 Å. Similar to the $(G8)_2$:$(LiAsF_6)_3$ complex, the three Li^+ ions and two glymes in the $(G9)_2$:$(LiAsF_6)_3$ form

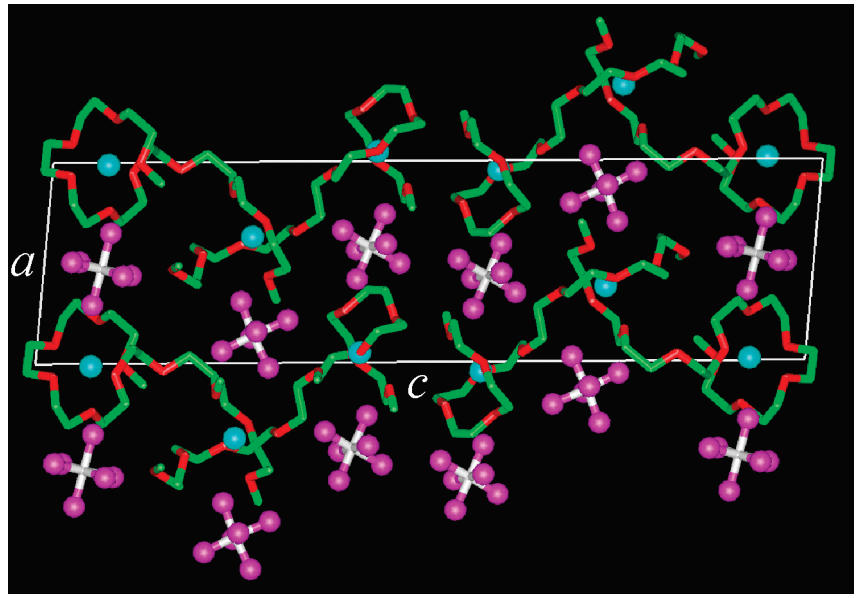

Figure 6. Structure of $(G9)_2$:$(LiAsF_6)_3$. Hydrogens not shown.

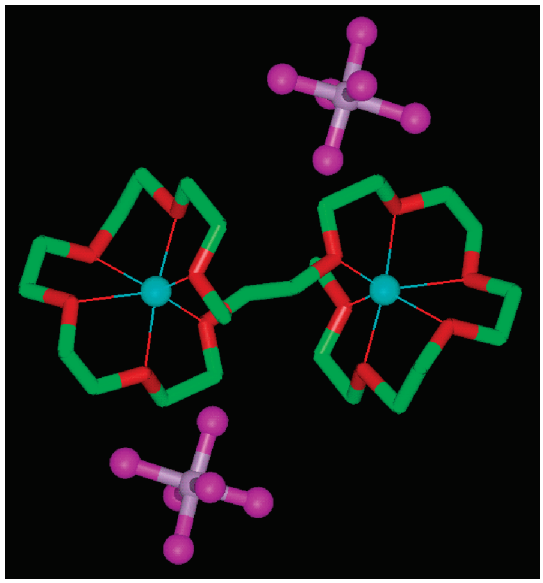

Figure 7. Local coordination environment of Li^+ ions in the structure of G11:$(LiAsF_6)_2$. Thin lines indicate coordination around the Li^+ cation. Hydrogens not shown.

a L-shaped solvate, Figure 5, with the middle lithium bridging the two nonaglymes. Two ether oxygens, one in each nonaglyme, are not involved in coordinating the lithiums. The lithium−lithium distances within the L-shaped solvate are, as expected, longer than in the 6:1 octaglyme complex, 6.87 and 7.84 Å.

Unlike the $(G8)_2$:$(LiAsF_6)_3$ complex, the L-shaped solvates in the $(G9)_2$:$(LiAsF_6)_3$ are stacked in columns in a chevron fashion along the *a* crystallographic axis, Figure 6. The Li^+-Li^+ distances between neighboring solvates are 9.22 Å along *a* and 7.18 Å at the closest point. The closest distance between lithiums belonging to neighboring columns is shorter, 6.42 Å.

The AsF_6^- ions are also stacked in columns along *a* separated by 9.22 Å. The shortest As−As distances between the columns of anions are 6.89 and 7.38 Å.

Structure of G11:$(LiAsF_6)_2$. As in the $(G8)_2$:$(LiAsF_6)_3$ complex, the oxygen to lithium ratio in the G11 complex is 6:1. Lithium ions are coordinated by six ether oxygens, with Li^+-O distances within the range 2.09−2.30 Å. Each undecaglyme molecule coordinates two Li^+ ions, forming a dumbbell-shaped solvate, Figure 7. The distance between lithium ions within the solvate is 6.70 Å.

The solvates and noncoordinating AsF_6^- ions are stacked in columns along the *b* crystallographic axis, Figure 8. The Li^+-Li^+ and As−As distance along the columns is 9.50 Å. In between columns lithium ions are separated by 6.81 Å and arsenics by 6.41−7.00 Å.

Structure of G12:(LiAsF6)2. The oxygen to lithium ratio in the complex is 6.5:1. Like in the G11:$(LiAsF_6)_2$ complex, lithium ions in G12:$(LiAsF_6)_2$ are coordinated by six ether oxygens, with Li^+-O distances within the range 2.06−2.25 Å. The middle oxygen of the dodecaglyme and the anions are not involved in coordination of the lithium. Similar to the undecaglyme complex, each dodecaglyme molecule coordinates two Li^+ ions, forming a dumbbell-shaped solvate, Figure 9. Due to the presence of an extra, compared to the G11:$(LiAsF_6)_2$ complex, EO unit in the middle of the solvate, the distance between lithium ions within the solvate in G12:$(LiAsF_6)_2$ is greater, 9.02 Å.

Similar to the undecaglyme complex, the solvates and anions in the G12:$(LiAsF_6)_2$ structure are stacked in columns, Figure 10. The Li^+-Li^+ distance along the columns is 6.60 Å and 9.02−14.98 Å between the columns. As in the undecaglyme complex, there are no apparent intermediate sites for the lithium ions to occupy in order to aid cation transport within the $(G12)_{1/2}$:$LiAsF_6$ structure. The shortest distance between neighboring arsenic atoms is 6.67 Å.

In the glyme:$LiAsF_6$ complexes, for which Li^+ ions are coordinated exclusively by ether oxygens, the coordination number is invariably 6. The same coordination number was also reported previously for the diglyme and tetraglyme complexes, for which Li^+ coordination is also exclusively by ether oxygens.[12,13] However, when a fluorine from an

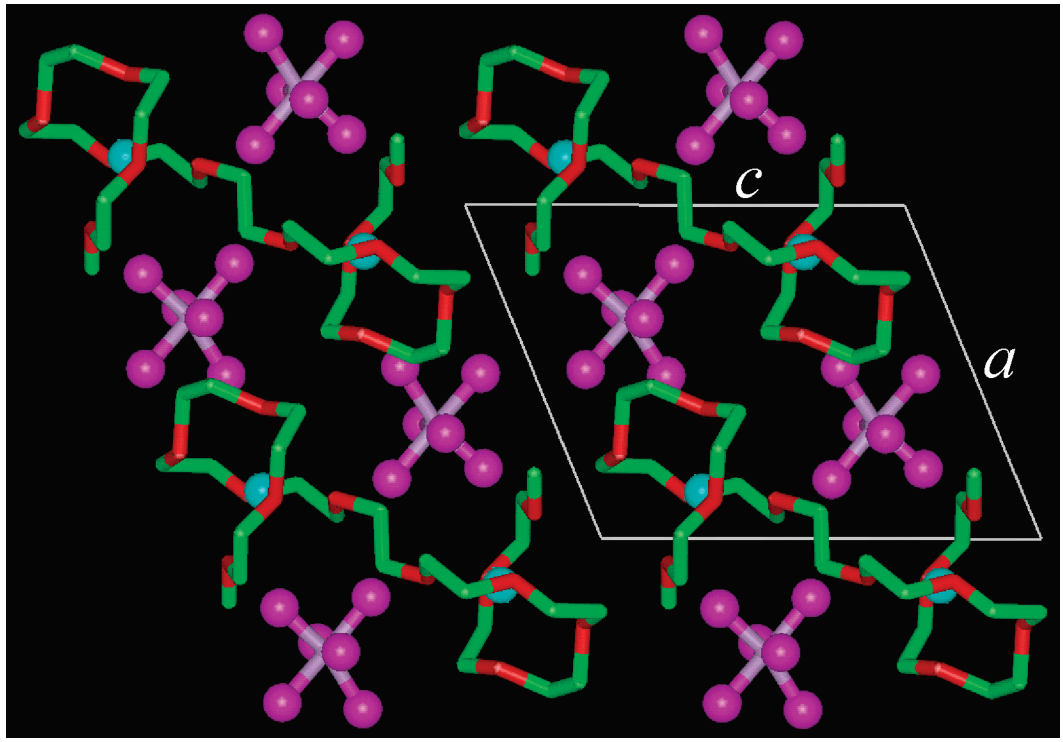

Figure 8. Structure of G11:$(LiAsF_6)_2$. Hydrogens not shown.

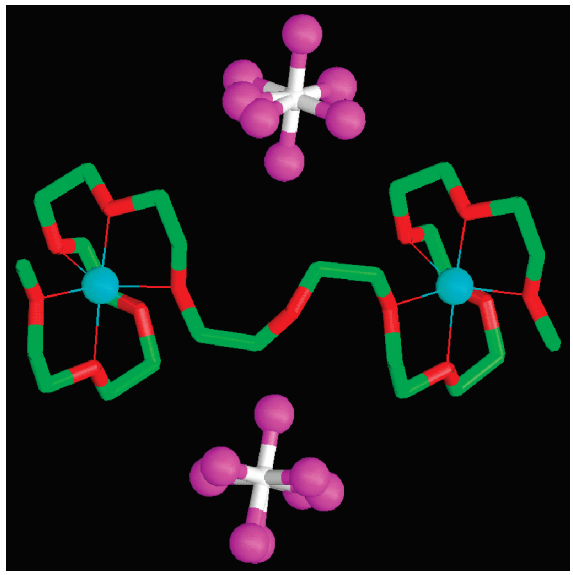

Figure 9. Local coordination environment of Li^+ ions in the structure of G12:$(LiAsF_6)_2$. Thin lines indicate coordination around the Li^+ cation. Hydrogens not shown.

AsF_6^- anion is involved in coordination, as in G8:$(LiAsF_6)_2$ and in the previously reported G3:$LiAsF_6$,[11] the coordination number is reduced to 5. Lower glymes (<G8) of different length (hence different number of oxygens) form complexes with very different crystal structures in order to ensure the required coordination number.[11–13] At the other extreme, when the number of EO units exceeds 22, the structure is invariant with molecular weight.[4] Complexes prepared with various higher glymes (G8−G12), although still forming a different structure when the molecular weight changes, have common structural features with their immediate neighbors, which have the same glyme/Li ratio. Typical examples of

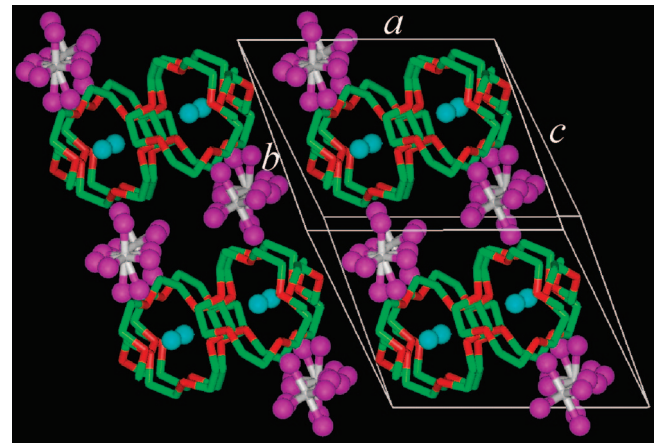

Figure 10. Structure of G12:$(LiAsF_6)_2$. Hydrogens not shown.

such similarities are L-shaped solvates in both $(G8)_2$:$(LiAsF_6)_3$ and $(G9)_2$:$(LiAsF_6)_3$ or the dumbbell-shaped conformation of the G11:$(LiAsF_6)_2$ and G12:$(LiAsF_6)_2$ glyme complexes.

The single-crystal data were collected at 93 or 173 K (see Supporting Information); however, the established structures are invariant with temperature, except for the change in lattice parameters due to thermal expansion, within the temperature range used in the conductivity measurements. The DSC traces (Figure 11) do not reveal any thermal events within the temperature range from 130 K to melting. Furthermore, the room-temperature experimental powder diffraction patterns match the patterns calculated from the structural models obtained at lower temperatures (see Supporting Information). The variation of conductivity with temperatures for the different complexes prepared with higher glymes is shown in Figure 12. Conductivities of the lower glymes have been reported previously.[17] Note that the conductivity of the

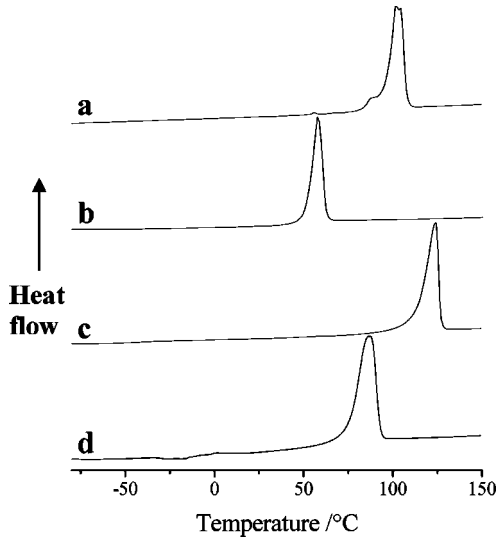

Figure 11. DSC data for (a) G8:$(LiAsF_6)_2$, (b) $(G9)_2$:$(LiAsF_6)_3$, (c) G11:$(LiAsF_6)_2$, and (d) G12:$(LiAsF_6)_2$.

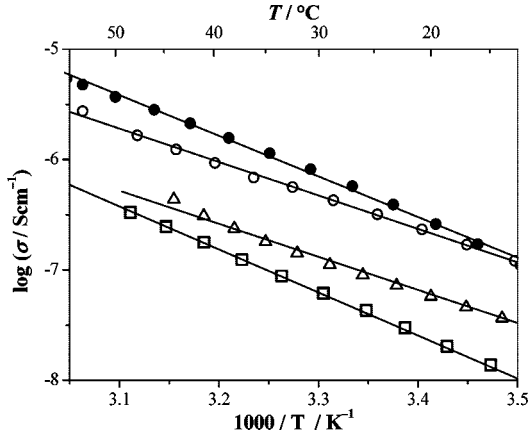

Figure 12. Ionic conductivity as a function of temperature of G8:$(LiAsF_6)_2$ (open squares), $(G9)_2$:$(LiAsF_6)_3$ (open triangles), G11:$(LiAsF_6)_2$ (filled circles), and G12:$(LiAsF_6)_2$ (open circles).

$(G8)_2$:$(LiAsF_6)_3$ is not reported because a single-phase powder of this complex could not be obtained. The linear variation of log σ versus $1/T$, as can be seen in Figure 12, is consistent with ion hopping between sites in all complexes. The slopes of the lines in Figure 12 indicate that the activation energy for the ion transport is similar for the G8−G12 complexes. The Li^+ transport number, t_+ (fraction of current carried by the cations), was determined following the procedure described in ref 10. The process included applying a dc polarization to the electrolyte and measuring the initial and steady state currents with corrections for the electrolyte/electrode interface using ac impedance, and the values were between 0.1 and 0.3.

The ionic conductivity of the G8−G12 complexes is lower than that of the G4:$(LiBF_4)_2$, G3:$LiAsF_6$, and G4:$LiAsF_6$.[10,19] The G4:$(LiBF_4)_2$ and G3:$LiAsF_6$ complexes are predominantly Li^+ conductors with a lithium transport number, t_+, of 0.7 and 0.8, respectively. The higher ionic conductivity of these two complexes can be explained by the presence of convenient pathways for the lithium ions to move within their crystal structures and by the shorter Li−Li distances along those pathways. The structures of the complexes with higher glymes presented here do not exhibit similar pathways for the Li^+ ions to move, which is supported by the low values of t_+ in these complexes, but they do provide routes for migration of the AsF_6^- anions. However, the conductivity of the higher glymes complexes is still inferior compared to that of the G4:$LiAsF_6$, which is predominantly an anionic conductor ($t_+ = 0.1$). This could be attributed to greater distances between adjacent AsF_6^- ions in the structures reported here (typically 6.4−7.3 Å) than in the G4:$LiAsF_6$, 6.0 Å. The longer distances between anions might make ion hopping between the neighboring anionic sites less frequent. There are shorter As−As distances, 5.8 Å, within the structure of G8:$(LiAsF_6)_2$, but one-half of the anions in that compound are involved in coordination of Li^+, which probably impedes their mobility.

Acknowledgment. P.G.B. is indebted to the EPSRC and the EU for financial support.

Supporting Information Available: X-ray crystallographic data files (CIFs); tables of crystal and refinement data and of selected bond lengths and bond angles, experimental and calculated from single crystal data powder diffraction patterns (PDF). This material is available free of charge via the Internet at http://pubs.acs.org.

CM8005327

(19) Zhang, C.; Ainsworth, D.; Andreev, Y. G.; Bruce, P. G. *J. Am. Chem. Soc.* **2007**, *129*, 8700.